

Finite-temperature thermophysical properties of fcc-Ca

N.K. Bhatt^{1,a}, P.R. Vyas¹, V.B. Gohel¹, and A.R. Jani^{2,b}

¹ Department of Physics, Gujarat University, Ahmedabad, 380 009, Gujarat, India

² Department of Physics, Sardar Patel University, Vallabh Vidyanagar, 388 120, Gujarat, India

Received 4 April 2007

Published online 13 July 2007 – © EDP Sciences, Società Italiana di Fisica, Springer-Verlag 2007

Abstract. At an extreme environment, such as high-temperature and high-pressure, harmonic theory has obvious limitations, where the anharmonic effects are influential in determining bulk properties of the materials. In this regard, necessity for incorporating anharmonicity through vibrational contribution and thermally excited electrons to the total free energy at finite temperatures is illustrated taking an example of divalent fcc-Ca. In this regard, we have employed a coupling scheme of combining recently proposed mean-field potential (MFP) with the local pseudopotential to obtain vibrational contribution to the total free energy. To access the applicability of the present coupling scheme, we have calculated temperature variation of several thermodynamical properties. Static EOS, shock Hugoniot and temperature along principal Hugoniot are also estimated. Results are satisfactorily compared with the other theoretical and experimental data and the use of local pseudopotential in conjunction with the MFP approach is justified.

PACS. 65.40.Ba Heat capacity – 65.40.De Thermal expansion; thermomechanical effects – 64.30.+t Equations of state of specific substances

1 Introduction

The properties study of materials at high pressures and high temperatures is always inevitable to extend our present understanding regarding the behaviour of the materials to these external influences as well as for the future technological developments. At an extreme environment, such as high-temperature and high-pressure, harmonic theory has obvious limitations, where the anharmonic effects are decisive in determining bulk properties. To account for anharmonic effects, which is essential otherwise to study the phenomena associated to structural phase transition, melting of materials and thermophysical properties at other than ambient conditions, lots of efforts have been made in past. Unfortunately, on one hand, experimentally, where anharmonic effects can be estimated by studying damping of phonons and frequency shifts but large uncertainties in these results are observed (for example, see Refs. [1–3]). On the other hand, theoretical investigations require proper account of lattice vibration and contribution from thermally excited electrons. For instance, the later contribution can be accounted for by using Mermin functional [4] within the density-functional theory (DFT), while the treatment of ion-motional to the Helmholtz free energy pose difficulty. Current computational developments to incorporate ionic vibrations to the

total free energy are two fold: (i) complete ab initio or first principles methods [5–7] and (ii) relatively simple analytical approaches [8–13]. Full ab initio calculations, though highly reliable, at high temperatures and high pressures being difficult, they are usually implemented using certain well-defined approximations. In the second scheme, as for the temperature dependence properties study, mean-field approximation remains a subject of preference for the theoretical physicist. The central issue of mean-field theory is to find the simpler way to model mean-field potential (MFP) seen by the vibrating lattice ions. In this regard; (i) the free volume theory [10] calculates the MFP from average of the empirically derived pair-wise potential, (ii) particle in a cell (PIC) model or simply the cell model [11] employs tight-binding (TB) total energy calculations to estimate MFP, where TB potential parameters were fitted to the first principles results, and (iii) recently proposed MFP approach due to Wang and his co-workers [12]. These authors have used first principles FP-LAPW method within GGA to evaluate 0 K cohesive energy, which in turn was used to obtain vibrational free energy.

The alkaline-earth metals, group-II in the periodic table, have large compressibility and phase diagrams strongly influenced by a nearly empty *d*-band lying in close proximity to the *sp*-valance band. The *d*-band occupation increases with increasing atomic number and with increasing pressure. In effect, pressure converts the

^a e-mail: bhattnisarg@hotmail.com

^b e-mail: janiar@rediffmail.com

alkaline-earth metals from an alkali metal-like to an early transition metal-like character. Surprisingly, finite temperatures and pressures thermodynamic properties for these metals are scarce in the literature, until recently, Katsnelson et al. [14, 15] have estimated the effects of anharmonicity in the lattice dynamics and thermodynamics of Sr and Ca. Recently, we [16] have combined MFP approach to local pseudopotential due to Fiolhais et al. [17] to estimate equations of states (both static as well as shock Hugoniot) and temperature variation of thermodynamic Grüneisen parameter (γ_{th}) of elemental Sr. For the complete assessment of the MFP in conjunction with the local pseudopotential to the thermodynamics of alkaline earth metals, in the present communication, we have calculated several thermodynamic properties of elemental fcc-Ca at finite temperatures. Our first objective is to see to what extent anharmonic effects is accounted for in the present calculations through monitoring bulk moduli (isothermal and adiabatic), specific heats, Helmholtz free energy, thermodynamic Grüneisen parameter etc. at elevated temperatures. Secondly, to calculate static and dynamic equation of state (EOS), and temperature along principal Hugoniot, which manifests themselves the influence of the empty d -band in close proximity to the Fermi surface to these properties.

2 Calculation

The Helmholtz free energy at an extreme environment, neglecting electron-phonon interaction, can be written as,

$$F(\Omega, T) = E_C(\Omega) + F_{ion}(\Omega, T) + F_{eg}(\Omega, T). \quad (1)$$

Static energy $E_C(\Omega)$ in equation (1) has been calculated in second-order pseudopotential formalism with the ‘‘evanescent’’ local pseudopotential due to Fiolhais et al. [17]. These authors have used two possible ways of determining potential parameters, namely (α and R), so-called ‘universal’ and ‘individual’ ones. Universal set of parameters were fixed by empirical R_S and Z only, while the individual ones were determined by fitting actual value of the valence interstitial electron number N_{int} apart from R_S and Z . Here, R is the core decay length, α is a positive parameter and R_S is the radius of the sphere containing one electron. Since this local pseudopotential was constructed directly in and for solid state, equilibrium bulk properties can be calculated more accurately with the individual set of parameters. Due to this observation we, in this paper, have used individual set of parameters. Following zero pressure condition, we have determined R_S and hence 0 K volume. $E_C(\Omega)$ is then used to evaluate vibrational free energy $F_{ion}(\Omega, T)$, through mean-field potential (MFP) approach due to Wang and Li [12]. As noted by Katsnelson et al. [14], for group-II metals, a ratio of Fourier component of pseudopotential to Fermi energy is rather small. And therefore, it may be expected that the description of thermodynamics of Ca can adequately be given with the present coupling scheme (i.e. local pseudopotential +

MFP). Based on the second order pseudopotential theory, E_C can be written as

$$E_C = Z(e_k + e_x + e_c) + E_{es} + E_p + E_{bs}. \quad (2)$$

First term of above equation, $Z(e_k + e_x + e_c)$, is known as uniform electron gas energy. Here, e_k , e_x and e_c represent the kinetic, exchange and correlation energies of the homogeneous electron gas of charge Z ($=2$). The second term is the electrostatic energy. E_p and E_{bs} are the first and second order band structure energies, respectively. We have used local pseudopotentials proposed by Fiolhais et al., which has the following form in q -space.

$$\omega_b(q) = \left(\frac{8\pi Z R^2}{\Omega} \right) \left[\frac{-1}{(qR)^2} + \frac{1}{[(qR)^2 + \alpha^2]} + \frac{2\alpha\beta}{[(qR)^2 + \alpha^2]^2} + \frac{2A}{[(qR)^2 + 1]^2} \right], \quad (3)$$

where parameters A and β are expressed in terms of α as,

$$\beta = \frac{(\alpha^3 - 2\alpha)}{4(\alpha^2 - 1)} \quad \text{and} \quad A = \left(\frac{\alpha^2}{2} - \alpha\beta \right).$$

For Ca, individual parameters are $\alpha = 3.264$ and $R = 0.540$ a.u. (see Ref. [17]). Now, screened pseudopotential can be calculated through the relation $v_{ion}(q) = \omega_b(q)/\varepsilon(q)$, where $\varepsilon(q)$ is the modified Lindhard function. $v_{ion}(q)$ is related to Hartree dielectric function, and exchange and correlation function [18], which accounts exchange and correlation interactions for the free electron gas. This in turn is used to evaluate second order correction to the cold energy (E_{bs}) and hence 0 K total energy E_C . In present study, main objective is to obtain thermodynamic properties of Ca at and above room temperature (i.e. $T > \theta_D$; the Debye temperature, for Ca $\theta_D = 230$ K), ionic motion can be treated classically. Under the mean-field approximation, vibrational free energy of the lattice ion can be written as,

$$F_{ion}(\Omega, T) = -k_B T \left[\left(\frac{3}{2} \right) \ln \left(\frac{mk_B T}{2\pi\hbar^2} \right) + \ln \{v_f(\Omega, T)\} \right], \quad (4)$$

where

$$v_f(\Omega, T) = 4\pi \int \exp \left[\frac{-g(r, \Omega)}{k_B T} \right] r^2 dr. \quad (5)$$

Here, m is the mass of the ion and $g(r, \Omega)$ in equation (4) is the mean-field potential (MFP). Following Wang and Li [12], the MFP in terms of the E_C (cold static energy) is written as follows:

$$g(r, \Omega) = \frac{1}{2} [E_C(R_0 + r) + E_C(R_0 - r) - 2E_C(R_0)] + \left(\frac{\lambda}{2} \right) \left(\frac{r}{R_0} \right) [E_C(R_0 + r) - E_C(R_0 - r)], \quad (6)$$

where r is the distance that the lattice ion deviates from its equilibrium position, R_0 is the lattice constant with respect to Ω and λ is an integer. Three different values for λ , i.e. -1 , 0 and $+1$, corresponds to three expressions for Grüneisen parameter given, respectively, by Slater [19], Dugdale and MacDonald [20] and that for the free volume theory [10] (see Ref. [12] for more details). The last term in equation (1) is the Helmholtz free energy due to thermal excitation of free electron gas, which can be written as,

$$F_{eg} = E_{eg} - TS_{eg}, \quad (7)$$

where E_{eg} is the free electron kinetic, exchange and correlation energies, which have already been included in E_C (see first term of Eq. (2)). The entropy contribution, S_{eg} , is given by [21],

$$S_{eg} = Z \left(\frac{\pi k_B}{k_F} \right)^2 T. \quad (8)$$

Having obtained total Helmholtz free energy, $F(\Omega, T)$, at each temperature with zero-pressure condition, we have obtained various thermodynamic properties by standard thermodynamic equations (see, Ref. [13]), while shock Hugoniot is obtained through Rankine-Hugoniot conservation relation,

$$\frac{1}{2} P_H (\Omega_0 - \Omega_H) = (E_H - E_0). \quad (9)$$

Here, Ω_0 and E_0 refer to the atomic volume and energy at ambient conditions, respectively. Solving equation (9), one can easily derive the Hugoniot volume (Ω_H) versus pressure (P_H) as a function of known Hugoniot energy (E_H).

3 Results and discussion

Presently calculated 0 K binding energy ($E_{bin} = -1.48424$ Ry), fcc lattice constant ($R_0 = 10.7243$ a.u.), isothermal bulk modulus ($B_T = 15.641$ GPa) and its pressure derivative ($B'_T = 4.023$) are in close confirmation to the experimental results -1.4567 Ry (Ref. [22]), 10.545 a.u. (Ref. [22]), 15.2 GPa (Ref. [23]) and 3.9 (Ref. [24]), respectively. These all together can determine the 0 K energy curve, which in the present scheme, is essential to evaluate F_{ion} correctly. Shown in Figure 1, are the cold energy (0 K) versus lattice constants curve along with the Helmholtz free energies, at different temperatures nearly up to structural phase transition temperature, (for Ca it is $T = 726$ K), at which Ca transfers to bcc-phase. In alkaline metals like simple alkali metals, band energy varies much fewer thus depends more on volume than on crystal structure. Consequently, the stabilization energies are expected to be small for this group of metals, in contrast to those of transition metals. In this regard, the present simple scheme has obvious limitation to observe such a phase transition, and we have calculated thermophysical properties up to 700 K for fcc-phase. It is

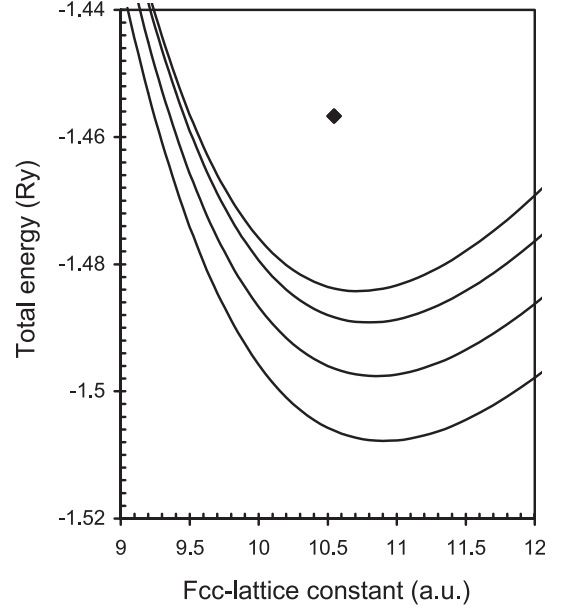


Fig. 1. The calculated total energy as a function of lattice constant for fcc-Ca. From top to bottom graphs correspond to temperatures, respectively, $T = 0$ K, 300 K, 500 K, and 700 K. Experimental point at $T = 0$ K is due to Kittel [22].

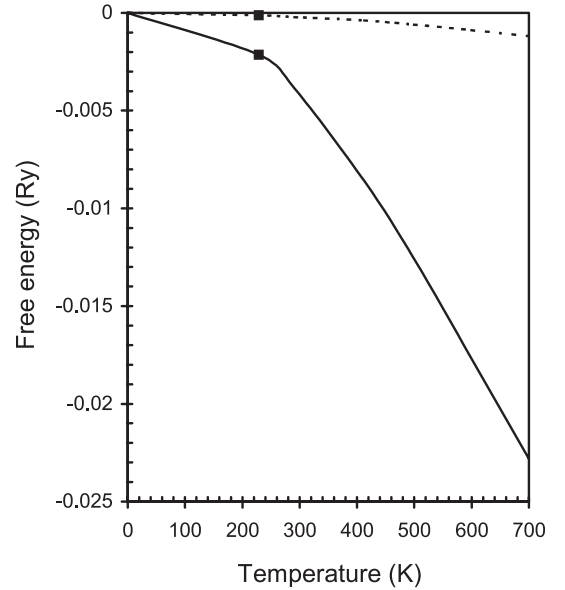


Fig. 2. Temperature variation of vibrational free energy (continuous line) and electronic free energy (broken line). Solid square corresponds to Debye temperature, for Ca $\theta_D = 230$ K.

obvious that at temperatures higher than Debye temperature ionic motion increases and leading to larger contributions to the total free energy. This can be inferred from Figure 2, where vibrational and electronic free energies are plotted against temperature. Free energy due to thermally excited electrons is found to be order of magnitude smaller than the ionic one. Solid square in the graphs corresponds to Debye temperature, above which lattice contributions become significant and F_{ion} increases rather rapidly.

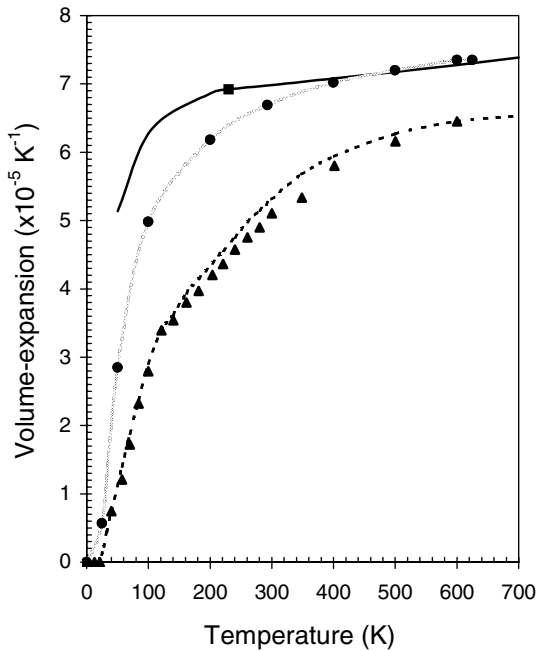


Fig. 3. Presently estimated volume-thermal expansion (continuous line) is compared with the experimental results: due to Touloukian et al. [25] (solid circles, while dotted line is the view to the eye) and Novikova [26] (solid triangles). Theoretical results due to Katsnelson et al. [14] is represented as broken line.

In harmonic theory inter-atomic potential energy is considered to be purely parabolic and therefore cannot predict thermal expansion. Asymmetry in the inter-atomic potential energy (i.e. anharmonicity) leads mean equilibrium separation to increase with temperatures. Figure 3 depicts results for volume-thermal expansion versus temperature along with the theoretical findings of Katsnelson et al. [14], and experimental results due to Touloukian et al. [25] (recommended values) and Novikova [26]. Katsnelson et al. [14] have separated electronic and lattice contributions to thermal expansion and fitted to the experimental results. Thus, they could estimate the phonon contribution to the thermal expansion as the difference of the experimental data and the electron contribution. This is shown in Figure 3. Also noted during the course of calculation that the thermal expansion is very sensitive to the choice of λ (see Eq. (6)), while equations of states remain almost unaltered. We have tried all three possibilities, and found that as λ moves from $-1 \rightarrow 0 \rightarrow +1$, volume-thermal expansion decreases. In the present calculation $\lambda = +1$ accounts better thermal expansion. At low temperatures ($T \ll \theta_D$), considerable departure from the experimental trend is seen, which is a typical feature of any finite-temperature calculations. All high-temperature calculations, till date, treat ionic motion classically and therefore are unable to account for quantum effects at low temperatures. Above Debye temperature, our results are in close proximity to the empirical results due to Touloukian et al. [25], and deviation at Debye temperature is about 9%, which decreases further with temperature. Since volume-thermal expansion is quite sensitive to the

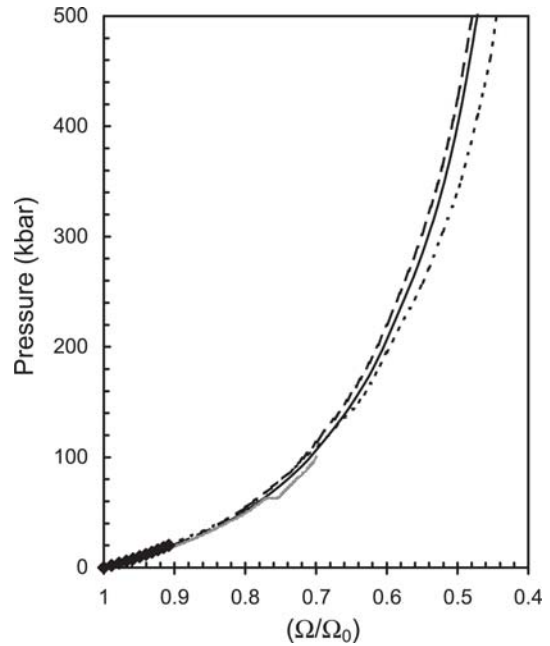


Fig. 4. Calculated isotherms at $T = 0$ K (broken line) and 300 K (continuous line). Experimental results: due to Bundy and Strong [27] (heavy dotted line at low pressures), solid diamonds are due to Anderson et al. [24]. Ab initio results (dotted line at $T = 0$ K) are due to Jona and Marcus [28].

microscopic dynamical quantities such as phonon frequencies, mode Grüneisen parameter and concavity parameter (where later describes the deviation from the linear behavior of the volume dependence of the phonon frequencies), good results for volume-thermal expansion at high temperatures reveal that the present scheme correctly takes care of these physical quantities.

Equations of states (EOS) have great importance in materials science. Static EOS at ambient temperature, which is largely governed by cold or 0 K total energy, provides a link to monitor microscopic internal structure of the material. Like-wise, dynamic or shock Hugoniot EOS gives information on the behaviour of the material, simultaneously, at high-pressure and high-temperature. Static EOS at 0 K and 300 K, and shock Hugoniot are shown in Figures 4 and 5, respectively. Experimental results for static EOS due to Bundy and Strong [27], those due to Anderson et al. [24] and recent first principles results (at $T = 0$ K) due to Jona and Marcus [28] are also shown for comparison. Jona and Marcus have calculated equilibrium properties of heavy alkaline metals, namely Ca, Sr and Ba, under hydrostatic pressures. Including zero-point energy with a generalized Debye approximation, these authors have estimated phase-transition pressures, elastic constants and static EOS for different crystal structures. It is clear from their results, for Ca, that pressures up to 500 kbar EOS in both bcc- and fcc-phase are almost identical. Thus, we have compared our results considering only fcc-phase with their corresponding findings. At highest pressure, departure of 17% with the results of Jona and Marcus has been found. Anderson et al. [24] have

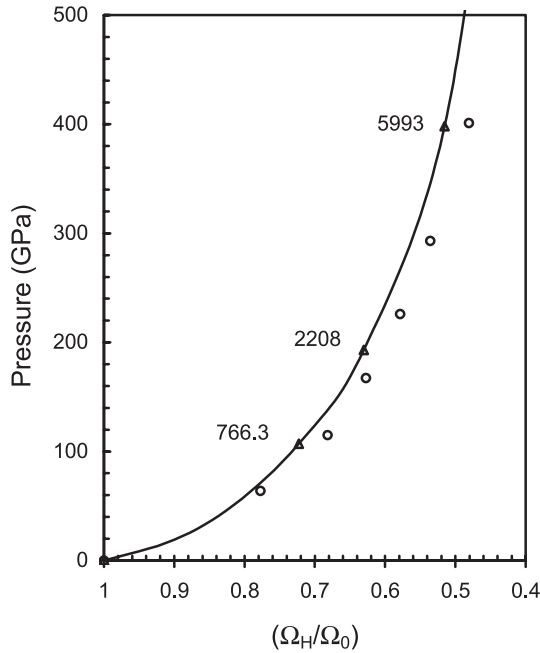


Fig. 5. Presently calculated shock-Hugoniot (continuous line), while the numbers besides triangles represent the estimated Hugoniot temperatures. Results due to Bakanova and dudoladov [30] are shown as open circles.

predicted negative pressure at $T = 0$ K, and at equilibrium volume. To include the effect of temperature, these authors have constructed empirical EOS with the adjustable parameters and deduce EOS (isotherm) at $T = 295$ K. Presently calculated results are in good agreement with these experimental data and maximum deviation of about 2.5% at 100 kbar is obtained. However, the structural phase transition (SPT) at 63 kbar observed in the results of Bundy and Strong [27] cannot be reproduced by the present scheme. This is in contradiction to more recent results on high-pressure EOS (see Ref. [29]), which predicts first SPT at 195 kbar (19.5 GPa), in which a crystal undergoes a first-order transition from one crystal structure (fcc – cF4) into another (bcc – cI2). Also shown in Figure 5 is the shock Hugoniot and temperature along principal Hugoniot with the experimental results due to Bakanova and Dudoladov [30] (open circles). Reasonable comparison is obtained with these data; nevertheless results in Figure 5 strongly support the validity of the Rankine-Hugoniot equation.

As a further test of the present approach to the zero-pressure properties, our calculated isothermal and adiabatic bulk moduli (B_T and B_S) versus temperature is compared in Figure 6 with the theoretical results due to MacDonald and MacDonald [31], Pandya [32], and experimental value due to Kittel [22] at $T = 0$ K and those due to Anderson et al. [24]. Difference of (almost constant) 15% is obtained with the empirical results of Anderson et al., and as expected, due to thermal expansion, bulk moduli decrease at higher temperatures. Ours as well as the results due to MacDonald and MacDonald [31] clearly justifies this fact, where their results overestimate the ex-

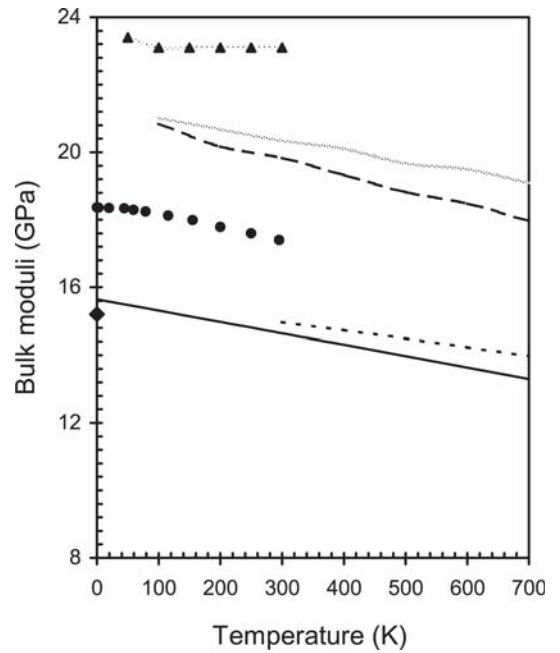


Fig. 6. Temperature variation of bulk moduli (continuous line for B_T and broken line is for B_S). Theoretical results: due to MacDonald and MacDonald [31] (long-dashed line for B_T , dotted line for B_S), due to Pandya [32] for B_T (Triangles with dotted line). Experimental values for B_T : due to Kittel [22] (solid diamond) at $T = 0$ K and those due to Anderson et al. [24] (solid circles).

perimental ones while ours underestimate the same for entire range of temperature that studied. These authors have calculated the Helmholtz free energy for a monatomic fcc crystal model assuming nearest-neighbour central-force (NNCF) interactions among atoms. They have included static lattice energy, and vibrational contributions from the harmonic and lowest-order, cubic and quartic, anharmonic terms in total Helmholtz free energy using perturbation theory evaluated in the high-temperature limit. They have employed modified Morse potential to represent pair potential, whose parameters were determined by fitting to sublimation energy and Debye temperature. For better quantitative agreement for the physical properties considered, they have refitted these parameters to linear-thermal expansion during the course of the calculation in the neighbourhood of the Debye temperature. It is to be noted, however, that no such fitting/refitting is made in the present calculations, except following zero pressure condition. Pandya [32] have considered Harrison’s generalized orthogonalized plane wave (OPW) pseudopotential method to extend it to study the d -band metals. He proposed a relatively simple form of pseudopotential, which takes $s - d$ hybridization effects into account in a parametric way. The author has evaluated free energy within harmonic approximation and thence different thermophysical properties (for instance, see Refs. [33,34]). Experimental trend (i.e. decrease in B_T with temperature) in his results is very weakly observed and also predicted values for B_T are too high compare to the experimental

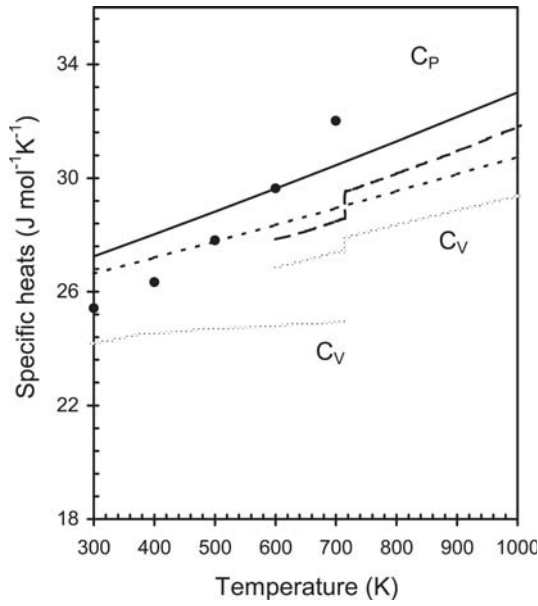


Fig. 7. Results for specific heats: C_P (continuous line) and C_V (broken line) are compared with the theoretical results due to Katsnelson et al. [15]: C_P (long-dashed line) and C_V (dotted line); while results from reference [14], for C_V (dotted line), is also shown, lower graph. Experimental data due to Hultgren et al. [35] for C_P are shown as solid circles.

values. Their results clearly reveal inadequacy of harmonic approximation above Debye temperature.

Shown in Figure 7 are the results for specific heats (C_P and C_V) at high temperatures with the other theoretical and experimental data. In the early paper, Katsnelson et al. [14], employing Animalu-Heine (AH) local pseudopotential within second-order perturbation approximation, have calculated lattice dynamics and various thermodynamic properties for Ca and Sr in both fcc- and bcc-phase close to melting temperature. Their results for C_V are shown for comparison as a lower graph in Figure 6. In this analysis, these authors have calculated heat capacity C_V through phonon density of states. They have separated lattice contributions from the experimental heat capacity and determined some momenta of phonon spectrum, while electron heat capacity (C_{el}) and contributions from thermally excited lattice defects, assuming very small, were neglected completely. Recognizing a fact that these contributions, though small, cannot be ignored at finite temperatures, later, they [15] have incorporated C_{el} evaluated from first principles method, namely FP-LMTO within LDA, and contribution from lattice defects in an approximate way. Incorporation of these anharmonic contributions has certainly improved their results qualitatively and quantitatively, which are also shown in Figure 6. Our results for C_V and C_P are in good proximity to these theoretical results and also to the experimental data [35] for C_P . Upward experimental trend for C_P cannot be observed in both the theoretical results, requiring further microscopic investigations. It is true that high-temperature martensite phase transition (MPT) (for Ca it is 726 K), usually accompanied by essential increase in the AE in

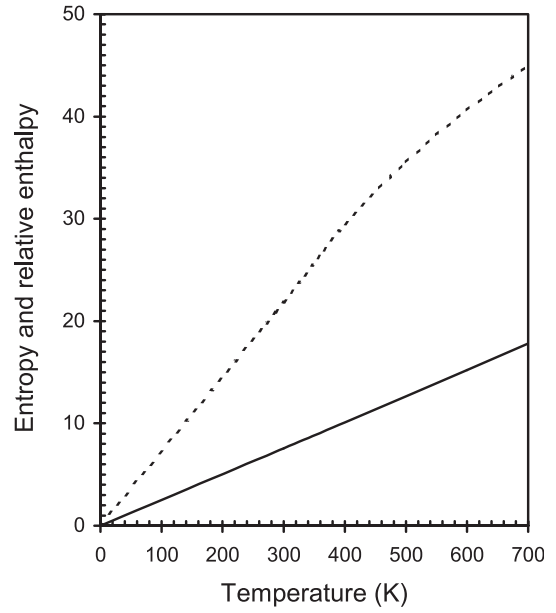


Fig. 8. Presently obtained entropy (broken line, in $\text{J mol}^{-1} \text{K}^{-1}$) and relative enthalpy (continuous line, in kJ mol^{-1}) is plotted against temperature.

lattice dynamics, is in controversy concerns the question whether MPTs are driven by soft phonons or by a different mechanism. In contrast to diffusive phase transitions the MPT is a collective phenomena; a signature of such transition cannot be reproduced by the present simple coupling scheme. Nevertheless, present scheme gives results, which are slightly better in agreement to the experimental data for C_P at higher temperatures (for instance, C_P at 700 K is 4.8% below to the experimental result) than the theoretical findings ($\sim 7.8\%$ at 700 K) due to Katsnelson et al. [15].

Estimated temperature variation of relative or scaled enthalpy (H) or zero-pressure internal energy (i.e. $H_T - H_0$) and entropy $S = (F - U)/T$ up to 700 K temperature is shown in Figure 7. In absence of other results we cannot compare our results with the other findings, but as expected, entropy and enthalpy increase with temperature for Ca.

Temperature dependence of thermodynamic Grüneisen parameter (γ_{th}), an important thermodynamic parameter often used to quantify the relationship between the thermal and elastic properties of a solid, is also obtained. According to Grüneisen, the volume dependence of the phonon frequencies can be estimated by the single parameter γ_{th} and thereby is the measure of the anharmonicity. His assumption about characteristic temperature for the phonon spectrum also means that this characteristic temperature depends only on volume and not on temperature at constant volume. Shown in Figure 8 is the temperature dependency of γ_{th} close to the melting temperature for fcc-Ca. Presently calculated results are underestimated to the experimental results (which we have quoted from the paper due to Katsnelson et al. [14]) as well as to the theoretical findings of

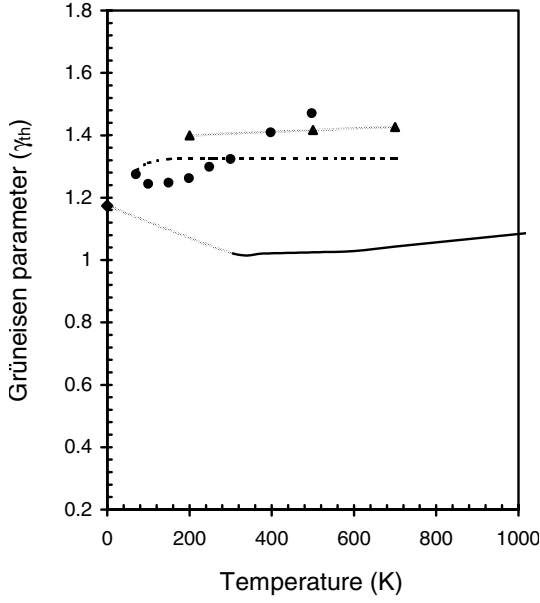


Fig. 9. Thermodynamic Grüneisen parameter as a function of temperature (continuous line), along with the theoretical findings of Katsnelson et al. [14] (broken line) and due to MacDonald and MacDonald [30] (triangles with dotted line). Experimental results (solid circles) are read from the respective graph from the paper due to Katsnelson et al. [14]. Solid diamond on the Y-axis is the estimated value for the same at $T = 0$ K, while dotted line is the view to the eye.

Katsnelson et al. [14] and those due to MacDonald and MacDonald [30]. Nevertheless, our results are consistent with the Grüneisen's assumption and increases weakly with temperature. Theoretical results due to Katsnelson et al. up to 700 K and those due to MacDonald and MacDonald using nearest-neighbour central-force (NNCF) model have the same temperature dependency. At $T = 0$ K, following Vashchenko and Zubarev [10], Grüneisen parameter can be written as,

$$\gamma_{th} = \frac{\frac{B'_T}{2} - \frac{5}{6} + \frac{2P}{3B_T}}{1 - \frac{4P}{3B_T}}$$

corresponding to $\lambda = +1$ (see for example, Burakovsky and Preston [36]). Here, B'_T is the pressure derivative of isothermal bulk modulus. This result is shown as a solid diamond on the Y-axis, while the hypothetical dotted line is the view to the eye. Having obtained volumetric expansion, isothermal bulk modulus, thermodynamic Grüneisen parameter, and specific heat at constant volume, one can also calculate temperature variation of $(\frac{\partial P}{\partial T})_V$, a quantity often of interest experimentally, as

$$\left(\frac{\partial P}{\partial T}\right)_V = \beta B_T = \frac{\gamma_{th} \cdot \Omega}{C_V}. \quad (10)$$

4 Conclusion

Importance and incorporation of anharmonicity through vibrational contribution and thermally excited electrons to the total free energy, which is essential otherwise to evaluate correctly thermophysical properties at high temperatures, is illustrated taking an example of divalent fcc-Ca. A simple conjunction scheme can yield results for thermophysical properties, which are in good agreement with the other ab initio theoretical and experimental data. Discrepancies seen in C_P at higher temperatures and thermodynamic Grüneisen parameter can be improved by incorporating contributions from lattice defects and vacancies, and, perhaps, through $s - d$ hybridization. Pollack et al. [37] have shown that calculated phonon frequencies with the same local pseudopotential are high in symmetric directions (particularly, phonon frequencies in L-branch along [100] and [111] directions are about 12% higher than the experimental ones) for Ca. Thus, possible improvement can be achieved, primarily for Grüneisen parameter, if pseudopotential parameters have been determined by fitting phonon frequencies as well. On the other hand, high-pressure static and dynamic equations of states are in reasonable agreement with the available experimental data. This can be improved further, again, by including $s - d$ hybridization. However, it is to be emphasized that, in the present calculations, once the potential parameters were determined at 0 K, during the progress of calculations no fitting/refitting to any of the experimental values in order to achieve quantitative results has been done and different thermodynamic properties were obtained consistently.

Thus, we conclude that (i) the pseudopotential due to Fiolhais et al. [17], which is controlled by three dominant parameters namely, the electron density, the valence Z and the density on the surface of the Wigner-Seitz cell, is found to be transferable to the other thermodynamic states (i.e. high-temperature and high-pressure states) without changing the values of the parameters and (ii) the present scheme (i.e. MFP + local pseudopotential), which bypasses lengthy and intricate computation, is proficient of producing results for thermodynamic properties in reasonable agreement with the observed results.

References

1. V.G. Vaks, S.P. Kravchuk, A.V. Trefilov, J. Phys. F: Met. Phys. **10**, 2105 (1980)
2. M. Zoli, G. Santoro, V. Bortolani, A.A. Maradudin, R.F. Wallis, Phys. Rev. B **41**, 7507 (1990)
3. M. Zoli, V. Bortolani, J. Phys.: Condens. Matter. **2**, 525 (1990)
4. N.D. Mermin, Phys. Rev. **137**, A1441 (1965)
5. D. Alfè, G. de Wijs, G. Kresse, M.J. Gillan, Int. J. Quant. Chem. **77**, 871 (2000); D. Alfè, G. de Wijs, G. Kresse, M.J. Gillan, J. Phys.: Condens. Matter **16**, S973 (2004)
6. V. Sorkin, E. Polturak, A. John, Phys. Rev. B **68**, 174102 (2003); V. Sorkin, E. Polturak, A. John, Phys. Rev. B **68**, 174103; S. Bernard, J.B. Maillet, Phys. Rev. B **66**, 012103 (2002)

7. J.A. Moriarty, Phys. Rev. B **38**, 3199 (1988); J.A. Moriarty, Phys. Rev. B **42**, 1609 (1990); J.A. Moriarty, Phys. Rev. B **45**, 2004 (1992); J.A. Moriarty, Phys. Rev. B **49**, 12431 (1994); J.A. Moriarty, Phys. Rev. B High Press. Res. **13**, 343 (1995)
8. V.V. Hung, K.M. Jindo, J. Phys. Soc. Jpn **99**, 2067 (2000); K.M. Jindo, V.V. Hung, Phys. Rev. B **67**, 094301 (2003)
9. V.L. Moruzzi, J.F. Janak, K. Schwarz, Phys. Rev. B **37**, 790 (1988)
10. V.Y. Vashchenko, V.N. Zubarev, Fiz. Trerd. Tale (Leningard) **3**, 886 (1963) [Sov. Phys. Solid State **5**, 653 (1963)]
11. L. Stixrude, R.E. Cohen, Science **267**, 8296 (1995); G. Steinle-Neumann et al., Nature **413**, 6851 (2001)
12. Y. Wang, L. Li, Phys Rev B **63**, 196 (2000); Y. Wang, R. Ahuja, B. Johansson, Phys. Rev. B **65**, 014104 (2001); Y. Wang, R. Ahuja, B. Johansson, J. Appl. Phys. **14**, 6616 (2002); Y. Wang, R. Ahuja, B. Johansson, Int. J. Quantum. Chem. **96**, 501 (2004)
13. N.K. Bhatt, P.R. Vyas, A.R. Jani, V.B. Gohel, J. Phys. Chem. Solids **66**, 797 (2005); N.K. Bhatt, P.R. Vyas, A.R. Jani, V.B. Gohel Physica B **357**, 259 (2005)
14. M.I. Katsnelson, A.V. Trefilov, M.N. Khlopkin, K.Y. Khromov, Phil. Mag. B **81**, 1893 (2001)
15. M.I. Katsnelson, A.F. Maksyutov, A.V. Trefilov, Phys. Lett. A **295**, 50 (2002)
16. P.R. Vyas, V.B. Gohel, N.K. Bhatt, A.R. Jani, Ind. J. Pure & Appl. Phys. **45**, 93 (2007)
17. C. Fiolhais, J.P. Perdew, Q. Armster, J.M. MacLaren, M. Brajczewska, Phys. Rev. B **51**, 14001 (1995); C. Fiolhais, J.P. Perdew, Q. Armster, J.M. MacLaren, M. Brajczewska **53**, 13193 E (1996)
18. J. Hubbard, Proc. Roy. Soc. A **243**, 336 (1957); L.J. Sham, Proc. Roy. Soc. A **283**, 33 (1965)
19. J.C. Slater, *Introduction to Chemical Physics* (McGraw-Hill, New York, 1939)
20. J.S. Dugdale, D.K.C. MacDonald, Phys. Rev. **89**, 832 (1953)
21. S.M. Osman, S.M. Mujibur Rahman, Mod. Phys. Lett. B **9**, 553 (1995)
22. C. Kittel, *Introduction to Solid State Physics* (Wiley, New York, 1996)
23. J.H. Rose, J.R. Smith, F. Guinea, J. Ferrante, Phys. Rev. B **29**, 2963 (1984)
24. M.S. Anderson, C.A. Swenson, D.T. Peterson, Phys. Rev. B **41**, 3329 (1990)
25. Y.S. Touloukian, R.K. Kirby, R.E. Taylor, P.D. Desai, *Thermophysical Properties of Matter* (Plenum, New York, 1975), Vol. **12**, p. 49
26. S.I. Novikova, *Thermal expansion of solids* (Nauka, Moscow, 1974)
27. F.P. Bundy, H.M. Strong, *Solid State Physics*, edited by F. Seitz, D. Turnbull (Academic Press, New York, 1962), Vol. **13**, p. 81
28. F. Jona, P.M. Marcus, J. Phys.: Condens. Matter **18**, 4623 (2006)
29. M. Winzenick, W.P. Holzapfel, Phys. Rev. B **53**, 2151 (1996)
30. A.A. Bakanova, I.P. Dudoladov, JETP Lett. **5**, 265 (1967)
31. R.A. MacDonald, W.M. MacDonald, Phys. Rev. B **24** 1715 (1981)
32. T.C. Pandya, Ph.D. Thesis, Gujarat University, India, 2000
33. C.V. Pandya, P.R. Vyas, T.C. Pandya et al., Physica B **307**, 138 (2001)
34. T.C. Pandya, P.R. Vyas, V.B. Gohel, Fizika (Zagreb) A **9**, 55 (2000)
35. R. Hultgren, R.D. Decai, D.T. Hawkins et al., *Selected Values of the Thermodynamic Properties of Metals and Alloys* (American society of metals, Cleveland, 1973)
36. L. Burakovsky, D.L. Preston, J. Phys. Chem. Solids **65**, 1581 (2004)
37. L. Pollack, J.P. Perdew, J. He, M. Marques, F. Nogueira, C. Fiolhais, Phys. Rev. B **55**, 15544 (1997)